Cortical network functional connectivity in the descent to sleep

Linda J. Larson-Prior[a,1], John M. Zempel[b], Tracy S. Nolan[a], Fred W. Prior[a], Abraham Z. Snyder[a,b], and Marcus E. Raichle[a,b,c,d,1]

[a]Department of Radiology, Washington University School of Medicine, 4525 Scott Avenue, St. Louis, MO 63110; [b]Department of Neurology, Washington University School of Medicine, St. Louis, MO 63110; [c]Department of Neuroscience, Washington University School of Medicine, St. Louis, MO 63110; and [d]Department of Biomedical Engineering, Washington University School of Engineering, St. Louis, MO 63130

Contributed by Marcus E. Raichle, January 28, 2009 (sent for review June 6, 2008)

Descent into sleep is accompanied by disengagement of the conscious brain from the external world. It follows that this process should be associated with reduced neural activity in regions of the brain known to mediate interaction with the environment. We examined blood oxygen dependent (BOLD) signal functional connectivity using conventional seed-based analyses in 3 primary sensory and 3 association networks as normal young adults transitioned from wakefulness to light sleep while lying immobile in the bore of a magnetic resonance imaging scanner. Functional connectivity was maintained in each network throughout all examined states of arousal. Indeed, correlations within the dorsal attention network modestly but significantly increased during light sleep compared to wakefulness. Moreover, our data suggest that neuronally mediated BOLD signal variance generally increases in light sleep. These results do not support the view that ongoing BOLD fluctuations primarily reflect unconstrained cognition. Rather, accumulating evidence supports the hypothesis that spontaneous BOLD fluctuations reflect processes that maintain the integrity of functional systems in the brain.

default network | fMRI | neuroimaging | non-rapid eye movement sleep

There is a physiologically distinct change in the state of the brain during sleep in comparison to wakefulness that is manifest subjectively as altered awareness and objectively as reduced responsiveness to environmental stimuli. The electrophysiological correlates of sleep are sufficiently pronounced and characteristic as to be defining (1, 2). Thus, natural sleep is characterized by a sequence of electroencephalographically defined stages that may be broadly divided into nonrapid eye movement (NREM) and rapid eye movement (REM) that cyclically alternate throughout the sleep period.

Over the past decade, PET studies have shown that throughout NREM sleep cerebral blood flow and metabolism are reduced in cortical association areas (3–7), as well as in the brainstem, thalamus, basal ganglia, and basal forebrain (3, 4, 7). NREM sleep is accompanied by reduced responsiveness to stimuli in regions involved in executive function, attention, and perceptual processing (5, 7, 8). The deepest NREM sleep states are characterized by low frequency oscillations in the EEG during which cognition is thought to be greatly reduced (9–13). During REM, cerebral blood flow and metabolism remain decreased in prefrontal and parietal regions but are increased in paralimbic areas, anterior cingulate, and thalamus (3, 7, 14), a pattern consistent with the emotionality and reduced logicality notable in during dreaming (7, 15, 16). REM sleep is also marked by atonia in skeletal muscles, reducing the ability to overtly respond to external stimulation. Thus, the transitions from wakefulness to successively deeper stages of NREM and then REM sleep progressively disengage the self from the environment.

It is now well-established that slow (<0.1 Hz) spontaneous fluctuations of the blood oxygen dependent (BOLD) signal show phase correlation in widely distributed functional networks (for review see ref. 17). The topography of these networks has proven to be highly consistent regardless of whether they are computed by correlation against selected seed regions (17–19) or by blind source separation methods (20–22). We here generically refer to all such methods as functional connectivity MRI (fcMRI). Remarkably, the networks obtained by fcMRI closely match the topographies of functional responses obtained by task-related fMRI using typical sensory, motor, and cognitive paradigms. Thus, fcMRI-defined networks appear to be highly stable.

The assumption that spontaneous BOLD fluctuations represent uncontrolled cognition follows naturally from the well-established relation between task-related responses and directed cognition. By measuring functional signal correlations in human subjects during the transition from wakefulness to sleep, we directly tested this idea.

Three higher order functional systems located within association cortices were selected for study: the dorsal attention system (23), which acts to focus perceptual processes on selected features of the environment (23, 24); the executive control system (25), which governs overt responses particularly in circumstances of complex and potentially conflicting contingencies; and the default system (26), which constitutes a set of regions in which activity is suppressed relative to quiet wakefulness during performance of externally oriented tasks. Current theoretical accounts of cognitive operations represented in the default system emphasize social cognition, episodic memory, and the construction of models of the external worlds (for a recent comprehensive review see ref. 27). We also examined fcMRI in 3 primary sensory systems (visual, auditory, and somatomotor). Should fcMRI measures primarily reflect mentation, descent into sleep should be accompanied by significantly reduced fcMRI in those networks supporting higher order cognition with no change seen in primary sensory systems.

Results

Ten healthy young adult subjects (22–24, 6 female) participated in these studies. Of these, 5 reached light NREM sleep during the course of the scan session. Two subjects returned for a second night, one of whom again attained light NREM sleep. Thus, our data set is composed of 6 sleep records and 5 nonsleep records.

Functional connectivity was examined using distributed network seeds (Table 1, see *Methods*). The purpose of this study was to evaluate defined functional networks for shifts in their interregional connectivity in 2 different brain states. Thus, we chose to evaluate each region of the defined networks against the average network activity pattern to obtain the strongest measure

Author contributions: L.J.L.-P. and M.E.R. designed research; L.J.L.-P., J.M.Z., and T.S.N. performed research; F.W.P. and A.Z.S. contributed new reagents/analytic tools ; L.J.L.-P., J.M.Z., F.W.P., and A.Z.S. analyzed data; and L.J.L.-P. wrote the paper.

The authors declare no conflict of interest.

[1]To whom correspondence may be addressed. E-mail: lindap@npg.wustl.edu or marc@npg.wustl.edu.

This article contains supporting information online at www.pnas.org/cgi/content/full/0900924106/DCSupplemental.

Table 1. Regional network seeds

Network	Seed region name	Talairach coordinates X	Y	Z
Default	**Posterior parietal/precuneus** (PCC) (19)	−2	−36	37
	Left medial prefrontal (LMPFC) (19)	−3	39	−2
	Right medial prefrontal (RMPFC) (19)	1	54	21
	Left lateral parietal (LLP) (19)	−47	−67	36
	Right lateral perietal (RLP) (19)	53	−67	36
Attention	**Left intraparietal sulcus** (LIPS) (19)	−23	−66	46
	Right intraparietal sulcus (RIPS) (19)	26	−58	52
	Left frontal eye fields (LFEF) (19)	−24	−12	61
	Right frontal eye fields (RFEF) (19)	28	−7	54
Sensory	Left auditory (LAud) (53)	−57	−14	12
	Right auditory (RAud) (53)	53	−16	13
	Left visual (LVC) (52)	−19	−96	−3
	Right visual (RVC) (52)	23	−96	1
	Right somatomotor (LSM) (54)	−39	−26	51
	Right somatomotor (RSM) (54)	38	−26	48
Executive Control	**Dorsal anterior cingulate** (dACC) (51)	−1	10	46
	Left operculum (LOP) (51)	−35	14	5
	Right operculum (ROP) (51)	36	16	4

ROIs used to create distributed network seeds are noted in bold. Numbers in parentheses are references.

of network, rather than regional, connectivity. Single seeded network connectivity was also evaluated, producing similar results to those found using the distributed network seed method (Figs. S1–S3). We found that all 3 higher order systems maintained their intra-system connectivity in light NREM sleep (Figs. 1 and S1). Further, these networks were consistent across subjects (Fig. 1).

Primary sensory systems show little reduction in energy metabolism or blood flow during light NREM sleep, and BOLD responses are similarly unaffected (3, 4, 28). We evaluated 3 primary sensory systems (Table 1) for changes in connectivity between wakefulness and light NREM sleep. As expected, these systems maintained their connectivity structure in early sleep, showing a consistent spatial pattern across subjects (Figs. 2 and S4).

While all systems examined maintained their interregional functional connectivity, the level at which this correlated activity was maintained differed between systems (Fig. S5). Indeed, the correlation values for the visual, auditory, and somatomotor regions of interest (ROI) remained statistically unchanged between wake and sleep (Fig. 2 and Figs. S3 and S5). Contrary to what one might predict, the dorsal attention network showed a significant increase in BOLD correlations in light NREM sleep relative to waking ($P \leq 0.015$, $n = 36$ [6 subjects, 6 ROIs]). As one might expect, the executive control network decreased in correlation strength in light sleep although this effect did not reach statistical significance ($P = 0.08$, $n = 18$ [6 subjects, 3 ROIs]). Interestingly, the default network, like the sensory systems, showed no change in its BOLD ($P = 0.83$, $n = 18$ [6 subjects, 3 ROIs]) correlation structure in light NREM sleep.

To verify that the distributed seed ROI technique generated reliable results, we repeated the computations using as a seed ROI the most prominent node in each functional system (dorsal attention = LIPS; default = PCC; control = LOP). This analysis replicated the main findings in all particulars (Fig. S2). Paired t tests again showed a significant increase in BOLD ($P = 0.03$, $n = 30$ [6 subjects, 5 ROIs]) correlation strength in dorsal attention network ROIs. The executive control network illustrated a nonsignificant reduction in correlation strength ($P = 0.3$, $n = 12$) and the default network was again unchanged in temporal ($P = 0.5$, $n = 18$ [6 subjects, 3 ROIs]) correlation strength.

It has been reported that significant differences in BOLD signal variance occur in NREM sleep (29, 30) that may represent

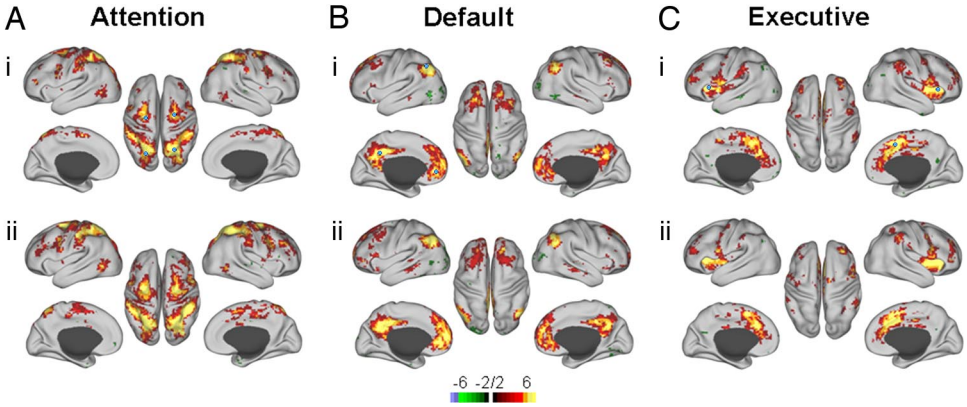

Fig. 1. Conjunction analysis of cognitive network seed correlations in wake (*i*) and light NREM sleep (*ii*). Seed ROIs are indicated by open circles (*i*) in all cases. There is wide-spread correspondence in the principal ROIs for each network across subjects ($n = 6$), and network connectivity is maintained in sleep for all networks.

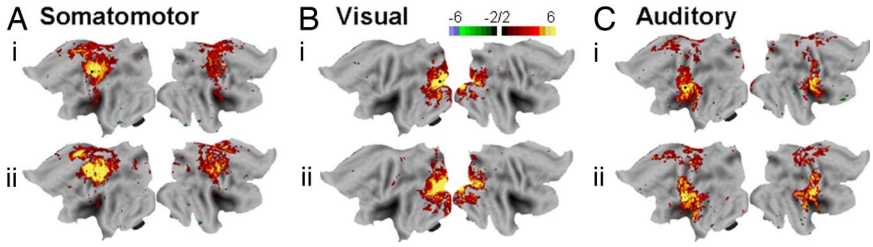

Fig. 2. Conjunction analysis of cross-hemispheric connectivity in sensory systems showing that connections are maintained in light NREM sleep. Seed regions (open circles) were created in the left sensory cortex (see Table 1) and show strong cross-hemispheric connectivity across all subjects ($n = 6$) in wake (*i*) that is maintained in sleep (*ii*).

a BOLD signature of sleepiness (30). These studies focused specifically on visual areas, which have been shown by others to be affected by eye closure during quiet waking rest (31), although increased signal fluctuation was also noted in whole brain. We evaluated changes in BOLD signal variance for both the whole brain signal regressed out of our functional connectivity analysis and for the variances in each ROI of our investigated systems. An overall increase in variance in sleep relative to waking was seen in the whole brain signal (Fig. 3*Ai*: wake 4.77 ± 2.0, sleep 5.59 ± 2.2, $n = 6$, $P \leq 0.1$). Signal variance in each cognitive system component ROI generally increased in light NREM sleep (Fig. 3*Aii*), although this did not reach statistical significance. The BOLD signal is illustrated for one subject in the transition from wake to light NREM sleep for the default network ROI and is typical of the level of signal variance in this transition for all systems analyzed (Fig. 3*B*). The observed changes in signal variance were not attributable to subject motion as subjects exhibited significantly less movement during sleep (0.41 ± 0.06 mm, $n = 7$) than in wake (0.69 ± 0.1 mm, $P \leq 0.0004$). It remains possible that the increase in whole brain BOLD signal variance reflects altered patterns of respiration (32).

We analyzed the BOLD spectral content to determine whether, like the EEG, it might exhibit a consistent shift in spectral content toward slower frequencies during the transition from waking to light NREM sleep (Fig. 3*C*). While there was a tendency for a shift to lower frequency content in BOLD in the descent to sleep in those systems that exhibited changes in functional connectivity strength, this was statistically nonsignificant when evaluated at 50 and 90% cumulative power (spectral edge) by network (parametric; $P > 0.14$ SE50, $P > 0.18$ SE90; nonparametric; $P > 0.44$ SE50, $P > 0.30$ SE90).

Discussion

The notion that the brain progressively disconnects from the external world as subjects fall asleep led us to hypothesize that measures of functional connectivity should similarly decrease in primary sensory and higher order cognitive systems if these measures reflect active information processing. However, while

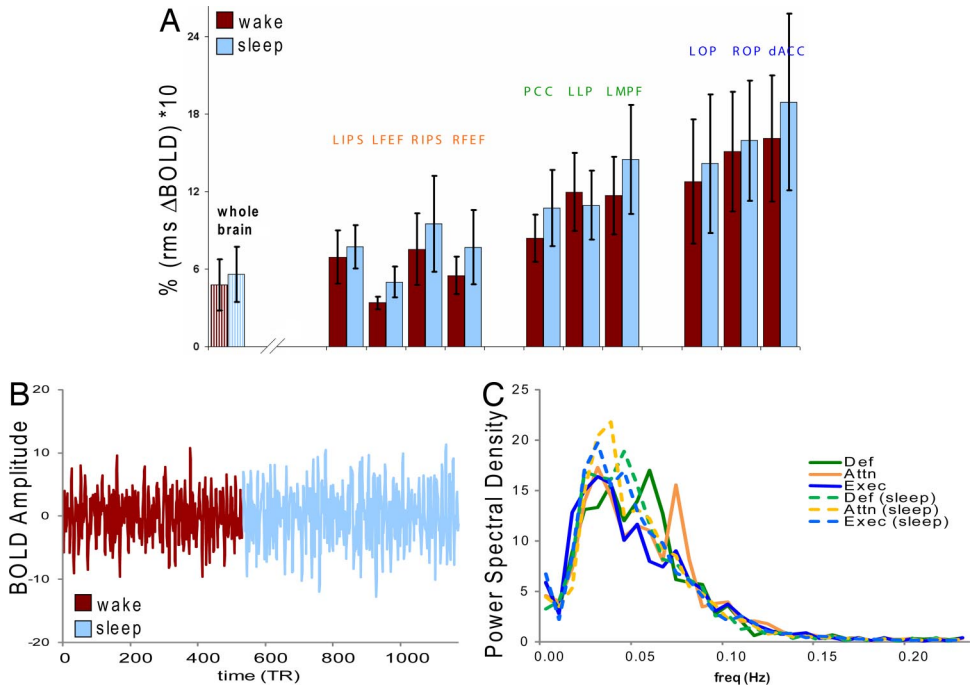

Fig. 3. BOLD signal variance was examined in the regressed whole brain signal (*Ai*, whole brain) and in each distributed network ROI following all regressions steps (*Aii*, solid bars). Whole brain signal variance showed a statistically significant increase with descent to sleep. There was a general trend toward increased signal variance in sleep (blue) relative to wake (red) in individual ROIs although this did not reach statistical significance. (*B*) A visual representation of the change in signal variance across state is illustrated. BOLD timecourses for each ROI in the default network are shown overlaid in the transition from wake (red) to sleep (blue). (*C*) Analysis of the BOLD spectral content demonstrates a general trend toward lower frequency bins in sleep (dashed lines) that was not statistically significant using either parametric (T, $P > 0.14$, SE50, $P > 0.18$, SE90, $n = 6$ per network) or nonparametric (Wilcoxon rank sum, $P > 0.44$ SE50, $P > 0.30$ SE90, $n = 6$ per network) methods.

there were some changes in functional connectivity in early NREM sleep, most systems exhibited little or no change. Thus, there was no evidence of reduced functional connectivity in the sensory (visual, auditory, and somatomotor) or cognitive networks (dorsal attention, default and executive control) examined. In particular the default network, widely associated with subjective awareness (33, 34), showed no measurable change in functional connectivity in the descent to sleep. It should be noted that our small sample size ($n = 6$) limits our ability to exclude quantitatively small changes; thus, to achieve an 80% confidence limit ($\alpha = 0.05$) for the observed effects size in the default network would require an additional 1000 subjects. The only change in functional connectivity was seen in the dorsal attention network, which (24) would arguably be the most likely to show reductions in network connectivity in sleep since it is known for its role in attention to the external environment. While power remained low ($d = 0.12$, 70% confidence limit, $\alpha = 0.05$), this network actually increased its connectivity. Despite the limitations in sample size, we are confident that if functional connectivity does change in early sleep, the magnitude of such changes is small. This is broadly consistent with previous reports on the effects of light sleep on network connectivity in humans (30). We conclude that the available data do not support the view that intrinsic BOLD fluctuations primarily reflect conscious mentation (17, 35). Rather, these intrinsic processes appear to exhibit quasi-structural properties that are preserved across levels of arousal.

Like sleep, anesthetic states are ones in which volitional cognitive processes are essentially abolished. Although representing distinctly different brain states, anesthetic states might be expected to produce reductions in interregional network connectivity. However, in keeping with the view that functional connectivity is preserved across levels of arousal, a recent study examining primate seed-based functional connectivity under isoflurane anesthesia (36) found that functional network connections based on spontaneous BOLD fluctuations were maintained under deep anesthesia.

Correlated activity within nodes of functional networks is necessary for the generation of normal functional organization during development (37–39). In addition, activity dependent changes in synaptic weighting are believed to underlie experiential learning throughout the life span, promoting the dynamic reconfiguration of neural networks to meet changing sensorimotor and cognitive processing demands (40–42). Sleep, particularly deep slow wave sleep, has been posited to represent a mechanism by which changes in synaptic weighting accumulated in wakefulness are homeostatically normalized (43, 44). Given the ubiquitous nature of such processes in establishing and dynamically regulating neural network activity, such correlated activity may also be necessary for the maintenance of functional organization throughout the lifespan.

Perhaps most intriguing is the difference in connection strength between the functional networks examined in this study. While the minimal change in cross-hemispheric sensory systems was anticipated, the statistical lack of change in the default network was surprising. Behaviorally, the default network was defined on the basis of its disengagement from active cognitive processing (26, 45), and others have reported reductions in metabolic activity and blood flow in states of reduced consciousness such as anesthesia (46, 47) and vegetative states (33) that are specific to a fronto-parietal network largely encompassing those regions that define the default network. Thus, given the loss of conscious volitional cognition represented by both sleep and anesthesia, both the default and attentional networks might logically be expected to reduce their connectivity in these states. The fact that this connectivity is maintained, even strengthened (as in the attentional network), suggests that the maintenance of connectivity in these networks is fundamental to brain function. The slight reduction in connectivity seen in the executive control network may reflect the well-known disengagement of executive control during sleep (6, 7).

Nonsignificant changes in BOLD signal variance in selected ROIs were seen in early NREM sleep along with a shift in BOLD spectral content toward lower frequencies (Fig. 3). These effects qualitatively correspond to very well known electrophysiological effects but they are much smaller in magnitude. Similar shifts in BOLD spectral power have been described in human subjects during anesthesia (48), where low frequency spectral power was reported to coincide with changes in intraregional correlation strengths. In our studies, these changes did not significantly correlate with state.

It is possible that larger sample sizes, descent to deeper NREM sleep, or REM sleep (where electrical activity more closely resembles that of wake), may result in clear changes in network connectivity. It is also possible that the abnormally restricted and noisy environment in which subjects slept affects connectivity in early sleep (for discussion, see *SI Methods*). However, the maintenance of functional networks under general anesthesia suggests that such connections, while they may change, will not be completely abolished. That the connectivity of interregional neural networks known to play a role in waking state function is maintained across all examined states of consciousness, suggests that maintenance of these network connections through ongoing spontaneous activity is of fundamental importance to the living brain.

Methods

Subjects. Ten right-handed, healthy human subjects (ages 22–54, 6 females) were recruited from the campus of Washington University under a protocol approved by the University's Human Studies Committee. All subjects gave informed consent and were compensated for their participation. Two subjects returned for a second sleep study.

Functional Imaging. Whole brain fMRI-BOLD (Siemens Allegra 3T scanner; TE = 30 ms, 4 mm^3 voxels, 2.013 sec/volume, 1 sec pause between frames) was acquired using an EPI sequence locally modified to enhance the signal/noise ratio. Structural data used for atlas transformations included a high resolution ($1 \times 1 \times 1.25$ mm) sagittal, T1-weighted magnetization-prepared rapid gradient-echo scan. fMRI runs were 20 min (398 volumes) in duration. Sleep latency, in most healthy subjects, falls within this time window (49). BOLD acquisition continued without interruption during interrun intervals (45 sec, 12 frames) needed to save the electroencephalographic (EEG) data to disk and restart recordings. This protocol ensured that subjects did not experience abrupt (arousing) changes in the auditory environment. Sleep sessions were conducted at night and included three to four 20 min runs. Sessions were terminated when subjects indicated that they were either unable to continue sleeping or were uncomfortable.

fMRI Data Preprocessing. fMRI data preprocessing included compensation of slice-dependent time shifts and elimination of intensity differences in even-odd slices resulting from interleaved acquisition, rigid body correction for interframe head motion, intensity scaling (to whole brain modal value of 1000), and atlas registration by affine transformation (50). Each fMRI run was transformed to atlas space and resampled to 3 mm^3 voxels.

Electroencephalography (EEG). Electroencephalography (EEG) data were acquired simultaneously with fMRI (DC-3500 Hz, 20 KHz sampling rate) using the MagLink™ (Compumedics Neuroscan) system (modified 10/20, 64 electrodes) and the Synamps/2™ amplifier. Sixty-four EEG leads were placed in an extended version of the International 10–20 system using the MagLink™ cap (Compumedics Neuroscan), including an external cardiac lead (In Vivo Research Inc.) that was used in a later artifact correction step, and bipolar vertical eye leads. Electrodes were referenced to an electrode placed 5 cm posterior to CZ. Gradient artifact and ballistocardiogram were reduced using Scan 4.5 and Curry 6.0 software respectively (Compumedics Neuroscan). Instantaneous power in 4 classic frequency bands (sigma, 11–15 Hz, alpha, 8–12 Hz; theta 4–8 Hz; delta, 1–4 Hz) was computed for a 15 electrode transverse bipolar montage and used to evaluate state transitions from wake to sleep in 30 sec epochs (see *SI Methods*). Data were also visually scored in 30 sec epochs by an experienced observer (J.M.Z.) Fig. S6 according to standard criteria (1, 2). The EEG was impacted by recording in the scanner bore and from artifact reduc-

tion, making it necessary to very carefully evaluate records for sleep depth (see Fig. S7, *SI Methods*).

Analysis. Functional connectivity was assessed using methods described previously (19). The seed regions used to produce these maps are noted in Table 1, with those ROIs used to construct distributed network seeds noted in BOLD type. Briefly, following regression of noise signals (whole brain signal, ventricular signal, and white matter signal) (see ref. 19), the averaged BOLD time series was extracted from 12 mm diameter spheric volumes centered on foci defined by Talairach coordinates (Table 1, Fig. S8). The extracted seed time series was then correlated to all other brain voxels to produce spatial correlation maps. Correlation coefficients from each unique tested pair were used to construct a correlation matrix used to evaluate correlations within and between identified networks during quiet waking and sleep (Fig. S3), where sleep was defined as those periods in which stable, stage 2 sleep was attained (14.7–37.6 min, see Table S1). Seeds defined for the task positive attention network (19) were centered on the intraparietal sulcus (IPS) and the frontal eye field (FEF) region. For the task negative (19) or default (26) network, seeds were centered on the medial prefrontal cortex (MPF), the lateral parietal cortex (LP), and the posterior cingulate/precuneus region (PCC). For the executive control network (51), seeds were centered on the dorsal anterior cingulate/medial superior frontal cortex (dACC) and on the bilateral insula/frontal opercular region (LOP and ROP). Three additional seeds representing a distributed network region of interest were also created for the default network (PCC+LLP+LMPF), the attention network (bilateral IPS +FEF), and the executive control network (dACC+LOP+ROP). Seed regions of interest were also constructed for primary visual (VC), auditory (Aud), and somatomotor (SM) cortices (VC, ref. 52; Aud, ref. 53; SM, ref. 54). Results were calculated as Fisher-z transformed correlation values and group data were evaluated using a random effects analysis. Data are displayed as conjunction maps to illustrate the degree of agreement in connectivity maps for each network.

Statistical Analysis. Random effects analyses were performed on fcMRI group data ($P = 0.01$, multiple comparison corrected) and displayed using in-house software. CARET brain mapping software (http://brainmap.wustl.edu/caret; ref. 55) and the PALS human cortical atlas (56) were used to create display maps based upon these spatial image maps. A repeated measures analysis of variance (MANOVA) was performed to assess the effect of state on network. This analysis yielded no significant effect of state F (5, 30)+0.342, $P + 0.6$. For cognitive networks, in which observations were not balanced, an analysis of variance (ANOVA) was performed with network, state, and the interaction between network and state as independent variables. A significant difference between networks was found [F (2, 71) = 61.08, $P < 0.001$], but there was no significant effect of state [F (1, 71)_0.28, $P = 0.6$] or the interaction of network and state [F (2, 71) = 0.403, $P = 0.67$] Planned comparisons of state in each network are reported as paired *t* tests. Group data were analyzed using JMP 7.0 (SAS Insititute, Inc.). For analyses of BOLD variance, BOLD time series data were extracted for seed and distributed seed ROI's from the default, executive, and attentional networks and power spectral density (psd) was calculated using an autocorrelation method and the mean psd was calculated across subjects for each ROI ($n = 6$ per network ROI). To clarify possible shifts in the distributions of the psd across state, the data were transformed to cumulative power plots for statistical testing of the spectral edge (SE), calculated at 50 (SE50), and 90 (SE90) percent cumulative power. Both parametric (Student's *t* test (T) and nonparametric (Wilcoxon signed rank) methods were used to assess statistical differences in psd between waking and sleep states for each network of interest.

ACKNOWLEDGMENTS. The authors thank Dr. C. Hildebolt for statistical assistance. This work was partially supported by National Institutes of Health Grant NS006833 to M.E.R.

1. Rechtshaffen A, Kales A (1968) *A Manual of Standardized Terminology, Techniques, and Scoring System for Sleep Stages of Human Subjects* (Brain Information Service/ Brain Res Inst., Univ. of California, Los Angeles).
2. Iber C, Ancoli-Israel S, Chesson AL, Quan SF (2007) *The AASM Manual for the Scoring of Sleep and Associated Events* (American Academy of Sleep Medicine, Westchester IL).
3. Braun AR, et al. (1997) Regional cerebral blood flow throughout the sleep-wake cycle. *Brain* 120:1173–1197.
4. Maquet P (2000) Functional neuroimaging of normal human sleep by positron emission tomography. *J Sleep Res* 9:207–231.
5. Kjaer TW, Law I, Wiltschiotz G, Paulson OB, Madsen PL (2002) Regional cerebral blood flow during light sleep—A H(2)(15)O-PET study. *J Sleep Res* 11:201–207.
6. Dang-Vu TT, et al. (2005) Cerebral correlates of delta waves during non-REM sleep revisited. *NeuroImage* 28:14–21.
7. Maquet P, et al. (2005) Human cognition during REM sleep and the activity profile within frontal and parietal cortices: A reappraisal of functional neuroimaging data. *Prog Brain Res* 150:219–226.
8. Portas CM, et al. (2000) Auditory processing across the sleep-wake cycle: Simultaneous EEG and fMRI monitoring in humans. *Neuron* 28:991–999.
9. Campbell KB, Colrain IM (2002) Event related potential measures of the inhibition of information processing: II. The sleep onset period. *Int J Psychophsyiol* 46:197–214.
10. Massimini M, et al. (2005) Breakdown of cortical effective connectivity during sleep. *Science* 309:2228–2231.
11. Steriade M, Nunez A, Amzica F (1993) Intracellular analysis of relations between the slow (<1 Hz) neocortical oscillation and other sleep rhythms of the electroencephalogram. *J Neurosci* 13:33252–33265.
12. Timofeev I, Steriade M (1997) Low frequency rhythms in the thalamus of intact-cortex and decorticated cats. *J Neurophysiol* 76:4152–4168.
13. Timofeev I, Grenier F, Bazhenov M, Sejnowski TJ, Steriade M (2000) Origin of slow cortical oscillations in deafferented cortical slabs. *Cereb Cortex* 10:1185–1199.
14. Nofzinger EA, et al. (2002) Human regional cerebral glucose metabolism during non-rapid eye movement sleep in relation to waking. *Brain* 125:1105–1115.
15. Hobson JA, Pace-Schott EF (2002) The cognitive neuroscience of sleep: Neuronal systems, consciousness and learning. *Nat Rev Neurosci* 3:679–693.
16. Schwartz S, Maquet P (2002) Sleep imaging and the neuro-psychological assessment of dreams. *Trends Cogn Sci* 6:23–30.
17. Fox MD, Raichle ME (2007) Spontaneous fluctuations in brain activity observed with functional magnetic resonance imaging. *Nat Rev Neurosci* 8:700–711.
18. Biswal B, Yetkin FZ, Haughton VM, Hyde JS (1995) Functional connectivity in the motor cortex of resting human brain using echo-planar MRI. *Magn Reson Med* 34:537–541.
19. Fox MD, et al. (2005) The human brain is intrinsically organized into dynamic, anticorrelated functional networks. *Proc Natl Acad Sci USA* 102:9673–9678.
20. Beckmann CF, DeLuca M, Devlin JT, Smith SM (2005) Investigations into resting-state connectivity using independent component analysis. *Philos Trans R Soc Lond B* 360:1001–1013.
21. Damoiseaux JS, et al. (2006) Consistent resting-state networks across healthy subjects. *Proc Natl Acad Sci USA* 103:13848–13853.
22. Mantini D, Perrucci MG, Del Gratta C, Romani GL, Corbetta M (2007) Electrophysiological signatures of resting state networks in the human brain. *Proc Natl Acad Sci USA* 104:13170–13175.
23. Corbetta M, Shulman GL (2002) Control of goal-directed and stimulus-driven attention in the brain. *Nat Rev Neurosci* 3:201–215.
24. Husain M, Nachev P (2007) Space and the partietal cortex. *Trends Cogn Sci* 11:30–36.
25. Doesenbach NUF, Fair DA, Cohen AL, Schlaggar BL, Petersen SE (2008) A dual-networks architecture of top-down control. *Trends Cogn Sci* 12:99–105.
26. Raichle ME, et al. (2001) A default mode of brain function. *Proc Natl Acad Sci USA* 98:676–682.
27. Buckner RL, Andrews-Hanna JR, Schacter DL (2008) The brain's default network: Anatomy, function, and relevance to disease. *Ann NY Acad Sci* 1124:1–38.
28. Czisch M, et al. (2002) Altered processing of acoustic stimuli during sleep: Reduced auditory activation and visual deactivation detected by a combined fMRI/EEG study. *NeuroImage* 16:251–258.
29. Fukunaga M, et al. (2006) Large-amplitude, spatially correlated fluctuations in BOLD fMRI signals during extended rest and early sleep stages. *Magn Reson Imaging* 24:979–992.
30. Horovitz SG, et al. (2007) Low frequency BOLD fluctuations during resting wakefulness and light sleep: A simultaneous EEG-fMRI study. *Hum Brain Mapp* 29:671–682.
31. McAvoy M, et al. (2008) Resting states affect spontaneous BOLD oscillations in sensory and paralimbic cortex. *J Neurophysiol* 100:922–931.
32. Birn RM, Diamond JB, Smith MA, Bandettini PA (2006) Separating respiratory-variation-related fluctuations from neuronal-activity-related fluctuations in fMRI. *NeuroImage* 31:1536–1548.
33. Laureys S (2005) The neural correlate of (un)awareness: Lessons from the vegetative state. *Trends Cogn Sci* 9:556–559.
34. Gusnard DA, Akbudak E, Shulman GL, Raichle ME (2001) Medial prefrontal cortex and self-referential mental activity: Relation to a default mode of brain function. *Proc Natl Acad Sci USA* 98:4259–4264.
35. Vincent JL, et al. (2006) Coherent spontaneous activity identifies a hippocampal-parietal memory network. *J Neurophysiol* 96:3517–3531.
36. Vincent JL et al. (2007) Intrinsic functional architecture in the anesthetized monkey brain. *Nature* 447:83–86.
37. Maffei A, Nelson SB, Turrigiano GG (2004) Selective reconfiguration of layer 4 visual cortical circuitry by visual deprivation. *Nat Neurosci* 12:1353–1359.
38. Lu W, Constantine-Paton M (2004) Eye opening rapidly induces synaptic potentiation and refinement. *Neuron* 43:237–249.
39. Butts DA, Kanold PO, Shatz CJ (2007) A burst-based ''Hebbian'' learning rule at retinogeniculate synapses links retinal waves to activity-dependent refinement. *PLoS Biol* 5:0651–0661.
40. Adani Y, Sagi D, Tsodyks M (2002) Context-enabled learning in the human visual system. *Nature* 415:790–793.
41. Hihara S, et al. (2006) Extension of corticocortical afferents into the anterior bank of the intraparietal sulcus by tool-use training in adult monkeys. *Neuropsychologia* 44:2636–2646.
42. Baeg EH, et al. (2007) Learning-induced enduring changes in functional connectivity among prefrontal cortical neurons. *J Neurosci* 27:909–918.

43. Tononi G, Cirelli C (2003) Sleep and synaptic homeostasis : A hypothesis. *Brain Res Bull* 62:143–150.
44. Tononi G, Cirelli C (2006) Sleep function and synaptic homeostasis. *Sleep Med Rev* 10:49–62.
45. Shulman GL, et al. (1997) Common blood flow changes across visual tasks: II. Decreases in cerebral cortex. *J Cognit Neurosci* 9:648–663.
46. Kaisti KK, et al. (2002) Effects of surgical levels of propofol and sevoflurance anesthesia on cerebral blood flow in healthy subjects studied with positron emission tomography. *Anesthesiology* 96:1358–1370.
47. Qiu M, Ramani R, Swetye M, Constable RT (2007) Spatial nonuniformity of the resting CBF and BOLD responses to sevoflurane: In vivo study of normal human subjects with magnetic resonance imaging. *Hum Brain Mapp*,10/1002/hbm. 20472.
48. Kiviniemi V, et al. (2005) Midazolam sedation increases fluctuation and synchrony of the resting brain BOLD signal. *Magn Reson Imaging* 23:53–537.
49. Johns MW (2000) Sensitivity and specificity of the multiple sleep latency test (MSLT); the maintenance of wakefulness test and the Epworth sleepiness scale: Failure of the MSLT as a gold standard. *J Sleep Res* 9:5–11.
50. Ojemann JG, et al. (1997) Anatomic localization and quantitative analysis of gradient refocused echo-planar fMRI susceptibility artifacts. *NeuroImage* 6:156–167.
51. Dosenbach NUF, et al. (2006) A core system for the implementation of task sets. *Neuron* 50:799–812.
52. Kang HC, Burgund ED, Lugar HM, Petersen SE, Schlaggar BL (2003) Comparison of functional activation foci in children and adults using a common stereotactic space. *NeuroImage* 19:16–28.
53. Lehmann C, et al. (2007) Dissociated lateralization of transient and sustained blood oxygen level-dependent signal components in human primary auditory cortex. *NeuroImage* 34:1637–1642.
54. Fox MD, Corbetta M, Snyder AZ, Vincent JL, Raichle ME (2006) Spontaneous neuronal activity distinguishes human dorsal and ventral attention systems. *Proc Natl Acad Sci USA* 103:10046–10051.
55. Van Essen D, et al. (2001) An integrated software suite for surface-based analyses of cerebral cortex. *J Am Med Inform Assoc* 41:1359–1378.
56. Van Essen DC (2005) A population-average, landmark- and surface-based (PALS) atlas of human cerebral cortex. *NeuroImage* 28:635–662.